

KATARZYNA KOZIEŁ ¹, ALEKSANDRA GAJDA ¹, MARTA SKIBA ¹,
NORBERT SKOCZYLAŚ ², ANNA PAJDAK ^{1*}

INFLUENCE OF GRAIN SIZE AND GAS PRESSURE ON DIFFUSION KINETICS AND CH₄ SORPTION ISOTHERM ON COAL

The paper presents research on the influence of grain size of selected coals and their structural parameters on the diffusion coefficient and methane sorption isotherms. Two coals from Polish hard coal mines, differing in the coal rank, were tested. Sorption isotherms for methane were determined. An unconventional sequence of pressures 0→0.1→0→0.5→0→1.5 MPa was employed to assess the speed of achieving sorption equilibrium at different pressures. The studies of CH₄ accumulation kinetics were performed on various grain classes of the tested coals. Both the sorption capacity of coal and the diffusion coefficient proved to be highly sensitive to the experimental methodology. Critical measurement parameters in terms of determining the diffusion coefficient concerning the assumptions of the Crank model were indicated. The influence of the equivalent radius of coal grain on the process kinetics was demonstrated. The stepwise pressure increase factor was examined in the context of minimising the impact of sorption isotherm non-linearity on the results. The importance of the width of the grain class of coals was determined to reduce their maceral inhomogeneities. These factors are the most common reason that makes it difficult to quantitatively compare diffusion coefficient values.

Keywords: coal; CH₄ sorption; diffusion kinetics; diffusion coefficient; pore structure

1. Introduction

The presence of methane in hard coal seams is a natural phenomenon. It forms in an oxygen-free environment as a result of the decomposition of organic matter under the influence of

¹ STRATA MECHANICS RESEARCH INSTITUTE OF THE POLISH ACADEMY OF SCIENCES, 27 REYMONTA STR., 30-059 KRAKÓW, POLAND

² AGH UNIVERSITY OF KRAKÓW, FACULTY OF GEOLOGY, GEOPHYSICS AND ENVIRONMENTAL PROTECTION, AL. MICKIEWICZA 30, 30-059 KRAKÓW, POLAND

* Corresponding author: pajdak@imgpan.pl



© 2024. The Author(s). This is an open-access article distributed under the terms of the Creative Commons Attribution-NonCommercial License (CC BY-NC 4.0, <https://creativecommons.org/licenses/by-nc/4.0/deed.en>) which permits the use, redistribution of the material in any medium or format, transforming and building upon the material, provided that the article is properly cited, the use is non-commercial, and no modifications or adaptations are made.

appropriate temperature and pressure. Coal is not (i.e., peat) the result of an almost completely oxygen-free environment (like hydrocarbon with theoretically O_2 less than 0.2 mg/l), at least deposition is much shallower than organic matter as a precursor for thermogenic HC. Extracting energy resources that contain methane, such as hard coal, brings not only benefits but also the risk of uncontrolled gas emissions into the atmosphere. According to the Intergovernmental Panel on Climate Change, the Global Warming Potential (GWP) of methane (CH_4) is 28 times higher than that of carbon dioxide (CO_2) over a hundred years. Worldwide environmental organisations recommend reducing the emission of this greenhouse gas (GHG) by discontinuing the exploitation of hard coal. However, for many countries, this poses a threat to their energy security. Hence, there is a need to capture methane emitted from hard coal in a controlled manner.

Mechanisms of fluid transport and gas sorption and diffusion depend on many factors. One of them is the value of the specific surface area and the width of the gaps in the coal. Specific surface area is a parameter that characterises the amount of external surface area of a solid (sorber) per its mass. In coal, gas is adsorbed most efficiently in the finest pores up to 2 nm in diameter. According to IUPAC, these are called micropores and ultramicropores (up to 0.8 nm). They also make up the largest share of the pore space of coal [1,2]. In micropores and small mesopores, gas adsorption processes take place, where the gases occupy most of the total interior surface area [1,2]. Larger mesopores and macropores function in coal as pores that transport adsorbate [3]. A crucial element influencing pore structure in coal and porosity is the maceral structure [4]. According to the literature [5], macerals of the inertinite group have the highest porosity, while those of the liptinite group have the lowest. These characteristics also affect the sorption capacity of coal. Vitrinite macerals contain a more extensive network of micropores than inertinite and thus have pores that can adsorb gas. On the other hand, in the macerals of inertinite there are numerous mesopores with diameters in the range of 2-50 nm [2].

The origin of coalbed methane can have several sources. Since coal is a sedimentary rock, these sources can be primary and microbial or thermogenic. They can also be mixed sources of methane [6]. The presence of methane of microbial origin is typical, mainly in low-rank coal. In high-rank coal, methane of mixed origin or secondary, late-maturity microbial gas is prevalent [7].

Rock mass methane drainage is the most efficient and effective approach toward controlling methane hazards, as it prevents and reduces the frequency of methane emissions, outflows into the working area and sudden outbursts of methane and rocks [8]. In [9], a new coal seam methane drainageability index (CMDI) was introduced for pre-drainage techniques in a working mine. In this approach, seventeen parameters were considered as the main factors affecting the methane drainage from the coal seam, and the interaction matrix based on the fuzzy rock engineering system (FRES) was used to study coal seam methane drainage ability.

The emission of methane from hard coal is a result of the coal-methane system's efforts to reach thermodynamic equilibrium. Considering the methane accumulation within the pore structure of coal and the symmetrical process of methane emission, the term "sorption" is often used in a broader context than the process's essence would suggest. Most researchers define sorption (and desorption) not only as a surface phenomenon but also as a series of processes of which it is the final stage [10]. When describing the process of gas accumulation within the sorber, the time factor is primarily determined by gas transport processes, namely filtration and diffusion. It is assumed that the diffusion transport of methane pertains to phenomena occurring within the coal's pore structure. The pore structure of coal is the essential reason that affects

methane diffusion [11]. Within the complex and diverse pore network, the transport of methane molecules has been described as the sum of several types of diffusion [12-16]. Generally, diffusion is considered a molecular phenomenon driven by the concentration gradient of adsorbed methane particles. Quantitative considerations start with Fick's second law [17] as the foundation [18]. The parameter that characterises the kinetics of methane accumulation or emission is the diffusion coefficient. Ideally, the diffusion coefficient's value should be a material constant characterising the coal-methane system under examination.

Numerous researchers have examined the correlation between coal's technical parameters and gas diffusion coefficients. Han et al. [19] investigated the impact of particle size on gas diffusion and found that as sample grain diameters increase, the effective diffusion coefficient for CH₄ and CO₂ unexpectedly rises. Long et al. [20] research suggests that coal's pore structure is crucial, with diffusion coefficients showing an upward trend as pore size increases. Xu et al. [21] explains the mechanism of gas diffusion-percolation in multi-scale pores, i.e., at the beginning of the flow, gas flows out from the large external pores first, from the surface inwards. Over time, the pore size through which gas flows gradually becomes smaller, the diffusion resistance gradually increases, and the apparent diffusion coefficient slowly decreases. Pan et al. [22] analysed moisture's influence on diffusion rates and observed a noticeable effect of moisture content on CH₄ diffusion rates. Numerous studies have explored the influence of various parameters, including thermodynamic factors, on diffusion coefficients. When it comes to pressure's effect on diffusion coefficients, international scientists have conducted numerical and molecular simulations to determine its impact. However, consensus remains elusive regarding whether the effective diffusion coefficient increases or decreases with rising pressure [23]. Even utilising similar models, some authors concluded that diffusion coefficients increase with pressure [24-26], while others proposed that pressure-dependent changes in diffusion coefficients are model-dependent [27]. These studies have also highlighted the role of adsorption pressure in determining effective diffusivity for methane. Staib et al. [28] briefly reviewed pressure's influence on diffusion coefficients and found that both primary and secondary diffusion coefficients decrease as pressure rises. Cui et al. [29] and Liu et al. [30] research indicated a decrease in the diffusion coefficient with increasing pressure, but emphasised its additional sensitivity to coal sorption. In contrast, Wang et al. [31] demonstrated inconclusive trends between diffusion coefficients and pressure in their studies. The authors [32-35] analysed the impact of temperature on diffusion coefficients, revealing an increase with rising temperature. Zhao et al. [36] explored the combined effect of temperature and pressure, finding that the diffusion coefficient rises with temperature, and pressure initially increases it before causing a subsequent decline. Beyond thermodynamic parameters, coal's petrographic composition might also influence the diffusion coefficient [37-40]. Adsul et al. [41] noted a positive correlation between diffusion rate and low to medium-ranking coals, while diffusion rates are suppressed in highly carbonised coals. [42] studies indicated that coals rich in inertinite exhibit faster gas diffusion compared to coals abundant in vitrinite.

The variety and quantity of variables affecting the determination of the diffusion coefficient are extensive. The process of ascertaining the diffusion coefficient, whether through experimentation or calculation, necessitates several assumptions. To linearise diffusion differential equations involving a sorption factor, the following prerequisites must be met:

- sorption follows the linear Henry isotherm,
- up to the initial moment $t < 0$, the grain is uniformly saturated and maintains equilibrium with the concentration of free gas encompassing the grain,

- at $t = 0$, an abrupt alteration in gas concentration around the grain prompts the initiation of desorption and sorbate transport processes,
- the coal material is homogeneous, implying the disparity in maceral composition and ash content among grains of different sizes is disregarded,
- grain composition within the sieved class is homogeneous,
- gas emanates from a spherical grain (or another regular shape),
- the process is isothermal,
- sorption and desorption processes occur rapidly enough that their durations can be ignored, causing the kinetics of gas release to depend exclusively on the kinetics of gas particle diffusion transport within the grain.

A variety of assumptions, including their characteristics, affect the potential for differences in diffusion coefficient values. Furthermore, variations in values can arise based on the chosen experimental or theoretical approach. This paper presents a series of experiments aimed at assessing the extent to which the diffusion coefficient can be regarded as a material constant. The study analysed the effect of individual assumptions in the diffusion model on the resulting deviations. Special consideration was given to the effects of grain size and gas pressure on diffusion kinetics and sorption isotherms.

2. Materials and methods

Two types of hard coal originating from the Upper Silesian Coal Basin region in Poland were subjected to testing. The samples were obtained from the KWK “Budryk” Hard Coal Mine (referred to as Coal D) and ZG “Sobieski” Mine (referred to as Coal B). Fig. 1 shows the location of the mines sampled.

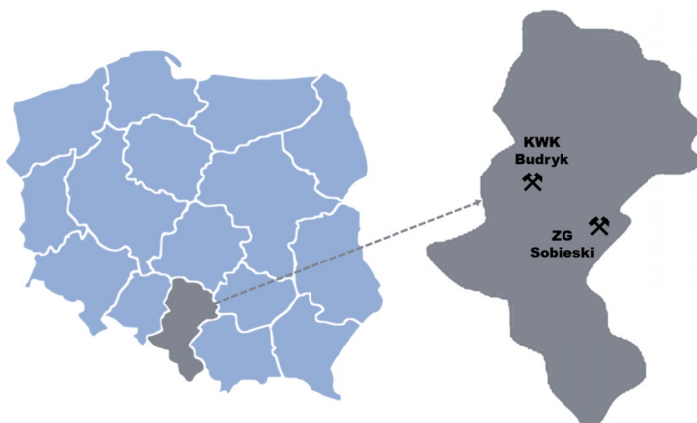


Fig. 1. Location of mines in Poland from which samples were taken for testing

Each coal sample was crushed and then sorted using sieves into grain classes of 0.16-0.25 mm, 0.25-0.5 mm, and 0.5-1.0 mm. The research process encompassed both auxiliary and primary

investigations. Auxiliary research involved determining petrographic and technical parameters, as well as structural characteristics pertaining to the coal's pore space arrangement. The primary research included sorption measurements conducted under high-pressure conditions following the author's designated methodology.

2.1. Materials

Technical analyses were conducted on coal's volatile matter and ash content based on Polish standards (PN-ISO 562:2000 and PN-ISO 1171:2002). The determination of maceral group content in the coal and the measurement of vitrinite reflectivity (R_r) were executed on polished grain preparations (briquettes) using white reflected light and an immersion liquid ($n_D = 1.518$ at 23°C) through an Axioskop (Zeiss) microscope. Petrographic composition analyses adhered to ISO 7404-3:2009 and ISO 7404-4:2017 standards. Reflectivity measurements were performed by ISO 7404-5:2009, involving either 100 or 500 measurement points. The data obtained was used to calculate the average reflectivity and standard deviation.

2.2. Structural parameters

Structural measurements were carried out using the ASAP 2020 (Micromeritics) low-pressure gas adsorption analyzer, utilising the volumetric method. The measurement involved determining the gas volume that occupied the open pores within the sample. Nitrogen (N_2) and carbon dioxide (CO_2) were employed as adsorbates. Measurements were conducted at temperatures of 77 K for N_2 and 273 K for CO_2 . Since the experiment was conducted under reduced pressure (0-0.1 MPa), it was assumed that the adsorbate occupied ultramicropores, micropores, and mesopores, wherein capillary condensation took place. Ahead of the N_2 adsorption measurement, the samples were degassed for 24 hours in an Ultra-High Vacuum (UHV) environment at 363K. Similarly, for CO_2 adsorption, the samples underwent 48 hours of degassing at 363K followed by an additional 4 hours at 368K.

The obtained sorption points as a function of pressure enabled the plotting of isotherms and the determination of structural parameters: specific surface area of the monolayer (Langmuir model) and multilayer (BET model), total pore volume, average pore size and pore size distribution (DFT theory and BJH model).

2.3. Sorption parameters

Sorption measurements were conducted using the gravimetric method with the IGA-001 device (Hiden Isochema) under high-pressure conditions. This apparatus records variations in sample mass during gas sorption by the porous material while accounting for gas buoyancy effects. The process is reflected as an augmentation in the mass of the sorbent-sorbate system. The sorbate was methane (CH_4). The gravimetric method is both isobaric and isothermal. The sorption testing procedure each time included:

- a) sample preparation:
 - selection of one of the 3 coal grain classes,
 - degassing of the coal sample under UHV conditions at a temperature of 353 K for no less than 24 hours for the lowest class and up to 120 hours for the highest grain class,

b) main measurement:

- quasi-step alteration of sorbate gas pressure in the reactor at a rate of 333 mbar/min,
- recording the mass changes within the coal-CH₄ system until sorption equilibrium is attained.

The measurement temperature was 313 K, while the measurement pressure was 0.1 MPa, 0.5 MPa and 1.5 MPa. Each successive sorption capacity measurement commenced with a vacuum stage.

Based on sorption points, by minimising the sum of squares of deviations, sorption isotherms were determined following the Langmuir model:

$$S(P) = \frac{A \cdot B \cdot P}{1 + B \cdot P} \quad (1)$$

where: $S(P)$ [mmol/g] is sorption equilibrium point, A [mmol/g] is total sorption capacity of the monolayer, B [1/MPa] is reciprocal of half pressure, P [MPa] is pressure.

2.4. Diffusion kinetics

Diffusion kinetics were analysed based on recorded changes in the mass of the coal sample during the CH₄ sorption process. This phenomenon is driven by the concentration gradient of gaseous sorbate in the pore space of the sorbent [43]. Methane seeks to equalise its concentration, as a result of which it is transported from the vicinity of coal grains towards the initially lower concentration within the pore structure. If, as a result of transport, a gas molecule comes within the range of intermolecular forces' interactions, its degrees of freedom are reduced, resulting in a change in the mass of the sorbent sample.

From a metrological perspective, this process is instantaneous. All the processes that contribute to the slow achievement of sorption equilibrium result from the molecular transport processes within the sorbent's pore structure.

The sorption process kinetics were interpreted as a reduction in the number of degrees of freedom for gas molecules adjacent to the sorbent surface. From a phenomenological perspective, this process is instantaneous. Any processes that lead to the gradual attainment of sorption equilibrium arise from the transport of molecules within the sorbent's pore structure.

In the kinetic description of the methane (CH₄) sorption/desorption process model on coal, the diffusion stage is presumed to be the predominant factor [44,45]. The parameter that quantifies diffusion kinetics is the effective diffusion coefficient. Its calculation enables the description of how the mass of the substance $M(t)$ accumulated in a spherical grain approaches the limiting value M_∞ . Determination of the value of the effective diffusion coefficient using the gravimetric method requires registered changes in the mass of the coal-methane system as a function of time after a step change in the pressure in the reactor.

In the combined processes of sorption and methane transport within coal, both mobile gas sorbate and bound sorbate coexist within the pore system. The transport occurs through the mobile sorbate, and the quantity of bound sorbate governs the adsorption rate. The accumulation process is assumed to transpire while upholding local sorption equilibrium, describable by the linear Henry isotherm. Initiated at $t = 0$ due to a step alteration in external conditions, these conditions remain constant. The accumulation process is accompanied by temporary alterations

in the distribution of the total sorbate concentration, C , within the grains. When assuming a linear sorption isotherm (Henry's isotherm – equation (2)), the progression of accumulation/emission can be described using Fick's second law (equation (3)):

$$S = H \cdot P \quad (2)$$

where: S [cm^3/g] is sorption capacity, H [–] is slope coefficient, P [bar] is pressure.

$$\frac{\partial c}{\partial t} = D_e \nabla^2 C \quad (3)$$

where: C [mol/m^3] is sorbate concentration, t [s] is time, D_e [m^2/s] is effective diffusion coefficient wherein:

$$D_e = \frac{D}{1+H} \quad (4)$$

where: D [m^2/s] is diffusion coefficient, H [–] is slope coefficient in Henry's sorption isotherm.

In equation (3), the diffusion coefficient D is substituted with the effective diffusion coefficient D_e . The value of this coefficient is derived from the diffusion coefficient D and the slope of the Henry isotherm. When analysing diffusion in spherical grains of radius R , equation (3) assumes the following form:

$$\frac{\partial u}{\partial t} = D_e \frac{\partial^2 u}{\partial r^2} \quad (5)$$

where: r [m] is the distance from the centre of the sphere, $C(r,t)$ [mol/m^3] is the distribution of sorbate concentration within it, wherein:

$$u = r \cdot C(r,t) \quad (6)$$

The solution to equation (3) takes the form:

$$\frac{C(r,t) - C_1}{C_0 - C_1} = 1 - \frac{2R}{\pi r} \sum_{n=1}^{\infty} \frac{(-1)^n}{n} \exp\left(-t \frac{D_e (\pi n)^2}{R_r^2}\right) \sin\left(r \frac{r \pi n}{R_r}\right) \quad (7)$$

where: C_1 and C_0 [mol/m^3] are constants determining the values of average concentrations of sorbate in the grain before and after the completion of the process, $M(t)$ [g] is the mass of the substance accumulated in the spherical grain approaches the limiting value M_∞ according to the formula:

$$\frac{M(t)}{M_\infty} = 1 - \frac{6}{\pi^2} \sum_1^{\infty} \exp\left(-\frac{n^2 \pi^2 D_e t}{R^2}\right) \quad (8)$$

where: M_∞ [g] is the total mass of gas accumulated in the grains, $M(t)$ [g] is the mass of gas accumulated at time t , R_r [cm] is the equivalent grain radius.

For a sample of the considered grain class, R_r is determined from the following relationship:

$$R_r = \frac{1}{2} \sqrt[3]{\frac{2 \cdot d_1^2 \cdot d_2^2}{d_1 + d_2}} \quad (9)$$

where: d_1 and d_2 [cm] are the grain size limits of the tested grain class.

When an isotherm other than the Henry isotherm is used, there is no analytical solution available for the problem, necessitating a numerical approach [46].

These relationships are described by Crank's unipore model [47]. Most of the assumptions of the Crank model are challenging to fulfil. The composition of grains within a specific class is not homogenous, and coal grains are not perfectly spherical. Additionally, at higher pressures, the shape of the sorption isotherm deviates noticeably from the linear Henry isotherm. Due to the inability to satisfy certain assumptions, the uncertainty of determining the effective diffusion coefficient might even reach several dozen percent.

Before the measurement, the sample was dried and evacuated under UHV conditions at 80°C for a duration necessary to stop the process of desorption of the gas naturally present in it. The actual initiation of the adsorption process, preceded by gas diffusion, started at the moment of abrupt pressure change in the reactor. To evaluate the effect of pressure on the process trajectory, the pressure was varied from deep vacuum to the analysed pressure. Subsequently, the sample was degassed again, following the same protocol as during its preparation. The subsequent experiment entailed a repeated step change in pressure from UHV to the next tested pressure value. Consequently, the experiment's procedure diverged from the classical concept where pressure changes assume successive values for individual sorption points.

In this article, diffusion kinetics was determined during all applied pressure changes. This approach was enabled by the specific pressure sequence employed: 0→0.1→0→0.5→0→1.5 MPa instead of the typical one: 0→0.1→0.5→1.5 MPa [48-51]. For the 0.5-1.0 mm grain class samples, the measurement procedure was time-consuming due to each time the sample was degassed in UHV. This time was symmetrical to the time needed to achieve sorption equilibrium.

3. Technical, petrographic and structural research

Coal samples from ZG "Sobieski" (referred to as Coal B) and KWK "Budryk" (referred to as Coal D) had different technical and maceral compositions. TABLE 1 contains the technical parameters of the tested coals. The contents of the microlithotypes and maceral composition are presented in TABLE 2. Coal from the "Sobieski" mine (Coal B) is classified as medium-rank B Meta bituminous coal, and coal from the "Budryk" mine (Coal D) as medium-rank D Para bituminous coal. According to the UN-ECE classification (UN-ECE, 1998), in terms of ash content, Coal B is classified as high-grade coal and Coal D as medium-grade coal. Coal B had a low coal rank, V_{daf} , about 76% (R_o about 0.56), while Coal D was correspondingly higher – 87% (R_o about 1.002).

Structural analyses encompassed the characterization of coal pore space through the utilisation of N_2 and CO_2 gases. In the analyses using nitrogen as the adsorbate, mainly the pore area in the mesopore range was characterised. The investigations spanned all three-grain fractions, and the findings are presented in TABLE 3. The obtained sorption isotherms had similar values,

TABLE 1

Technical parameters of coals

Origin	ZG Sobieski	KWK Budryk
Symbol	Coal B	Coal D
UN-ECE classification	medium-rank B Meta bituminous coal, high grade coal	medium-rank D Para bituminous coal, medium grade coal
Volatile content, V_{daf} (ash-free state) [%]	39.63	33.7
Ash content, ASH [%]	8.41	16.27
Moisture content, W_t [%]	5.35	1.37
Carbon content, C [%]	67.4	69.6
Sulphur content, St [%]	4.42	0.60
Hydrogen content, Ht [%]	4.64	4.30
Nitrogen content, N [%]	0.97	1.21
Vitrinite reflectivity, R_o [%]	0.57	1

TABLE 2

Petrographic parameters of coals

Parameter [% vol]	Grain class [mm]	Coal B	Coal D
Maceral composition: vitrinite/liptinite/inertinite	0.16-0.25	61.6 / 7.2 / 26.1	71.9 / 4.0 / 18.3
	0.25-0.5	62.0 / 7.0 / 25.8	72.4 / 4.2 / 18.0
	0.5-1.0	62.1 / 7.1 / 25.1	72.3 / 4.1 / 17.8
Vitrit		31.0	44.2
Inertite		2.0	3.8
Vitrinite		20.6	17.0
Clarite		8.8	10.8
Durite		2.4	0.6
Duroclarite		21.8	14.0
Vitrinertoliptite		2.0	—
Klarodurite		6.6	3.2
Carbominerite		3.2	4.4
Minerite		1.4	2.0

not exceeding 0.7 mmol/g in all samples (Fig. 2). In Coal B, specific surface area (BET) values ranging from 11.6 to 15.2 m²/g and pore volume (BJH) ranging from 18.2 to 12.8 mm³/g were obtained. For Coal D, these parameter values were comparatively lower, with specific surface area (BET) reaching up to 1.7 m²/g and pore volume reaching up to 5 mm³/g. The pore size distribution was established using the BJH model (Fig. 3). In both coals, the pore volume in the smallest coal granulation was higher than in the others. In Coal B, pores with diameters up to 10 nm prevailed, while in Coal D, no predominant range of pores was observed.

Nitrogen is very poorly sorbed within coal, leading to usually underestimated structural parameter results [52]. Moreover, these values often teeter on the brink of measurement uncertainties of the analyser. As a result, the analyses were repeated using carbon dioxide as an adsorbate. CO₂'s structure allows for effective penetration of fracture pores in coal, and the parameter

values derived from its use in coal tend to be close to real. Type I isotherms were obtained in all samples, and hysteresis was obtained in Coal D (Fig. 4).

TABLE 3

Structural parameters of coals

Sample	Coal B			Coal D		
	0-0.25	0.25-0.5	0.5-1	0-0.2	0.25-0.5	0.5-1
N_2						
BET surface area, m^2/g	11.6	14	15.2	1.7	1.1	0.8
BET total quantity adsorbed, cm^3/g	2.65	3.21	3.49	0.4	0.25	0.19
BJH volume of pores, mm^3/g	18.2	12.8	14.6	5	2.3	1.5
BJH average pore diameter, nm	8.3	7.6	7.6	15.4	12.8	12.8
CO_2						
Langmuir surface area, m^2/g	154.4	155.5	152.7	104.1	84.5	85.9
Langmuir total quantity adsorbed, cm^3/g	33.79	34.05	33.43	22.79	18.5	18.81
DFT total pore volume, mm^3/g	32.5	35.4	33.1	15.7	14.2	11.4

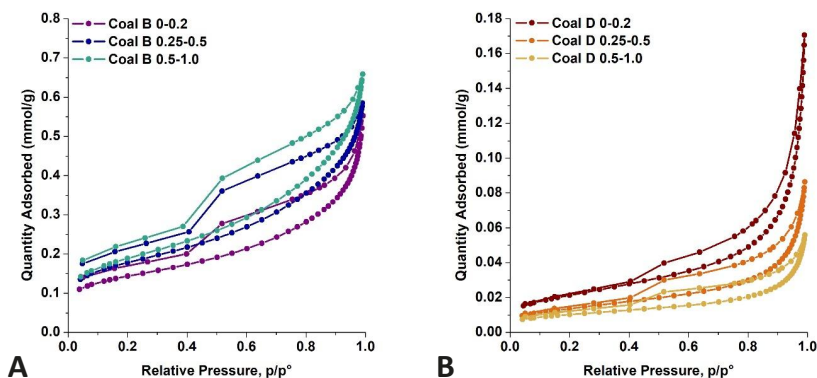


Fig. 2. N_2 sorption isotherms on coals of different grain size A) Coal B, B) Coal D

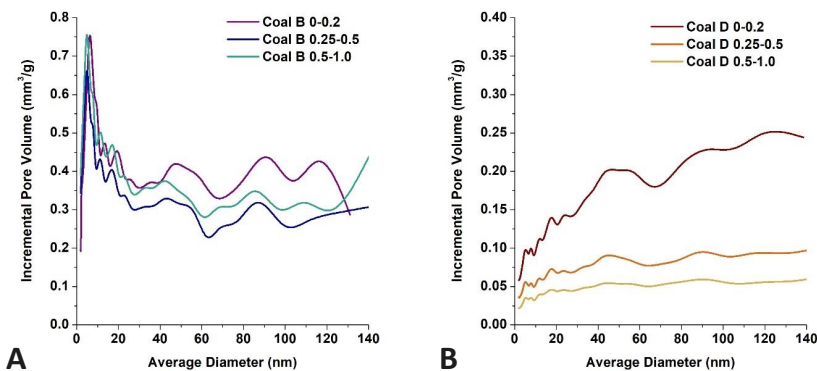


Fig. 3. Pore size distribution according to BJH model on coals of different grain size A) Coal B, B) Coal D

Since coal is primarily a microporous rock, the single-layer Langmuir surface filling model was used to describe its structural parameters. The specific surface area value (Langmuir) was about 153-155 m²/g, while for Coal D, it was 85-104 m²/g. This value in both coals was higher in finer grains.

Differences in specific surface area values between coals result from, among other factors, the maceral composition of the coals. Low-rank Coal B has a higher percentage of inertinite maceral, which is characterised by the most extensive structure and pore volume among all macerals [5]. The total pore volume determined using the DFT model dedicated to slit pores ranged between 32.5-35.4 mm³/g for Coal B and 11.4-15.7 mm³/g for Coal D, respectively (Fig. 5).

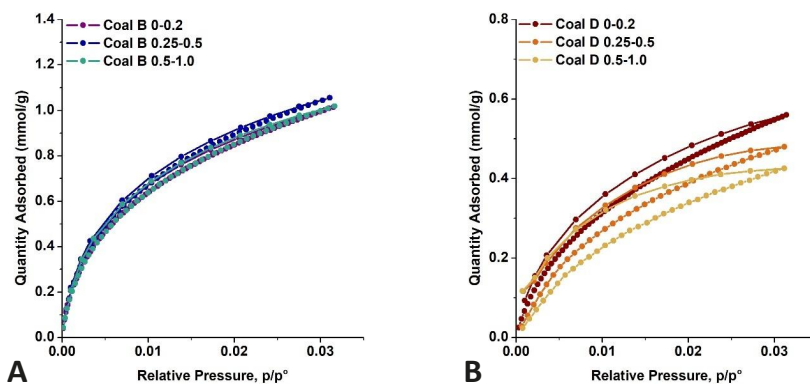


Fig. 4. CO₂ sorption isotherms on coals of different grain size A) Coal B, B) Coal D

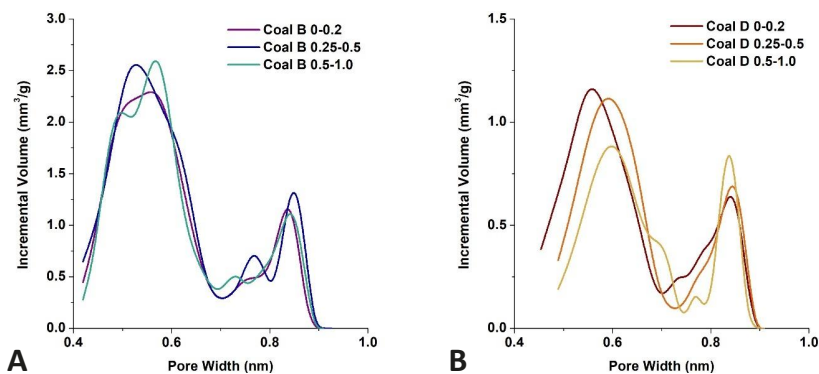


Fig. 5. Pore size distribution according to DFT model on coals of different grain size A) Coal B, B) Coal D

4. Measurements of sorption parameters

4.1. Sorption capacity

Determination of the CH₄ sorption capacity on Coal B was made for three-grain classes. For each of these grain classes, the replacement radius was determined following equation (9). In the

experiment, equilibrium sorption points were obtained at 1, 5 and 15 bar (Fig. 6A). The sorption capacity towards CH_4 was pressure-dependent. The higher the measurement pressure used, the higher the value of this parameter, which is consistent with the literature [48,54-56]. The highest values, about $18 \text{ cm}^3/\text{g}$, were obtained at 15 bar pressure. However, no significant differences were observed in CH_4 sorption capacity for individual replacement radii representing the successive tested grain classes. The average differences in the values were about $0.16\text{-}0.25 \text{ cm}^3/\text{g}$ per 0.01 cm of the increase in the replacement radius under the same pressure conditions. These relationships are shown in Fig. 6B. Based on the sorption points curve, the Langmuir sorption isotherm was adjusted, and the parameters of this isotherm were determined (equation (1)). Direct results of CH_4 sorption measurements on Coal B and calculations are presented in TABLE 4. The sample with the smallest grain size exhibited the highest Langmuir total sorption capacity.

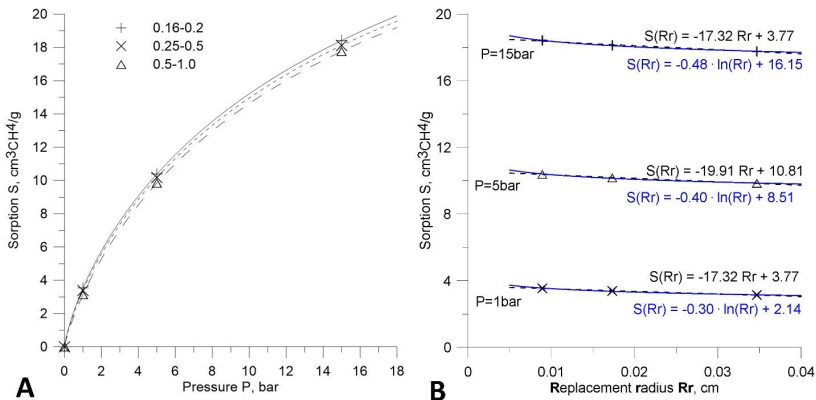


Fig. 6. CH_4 sorption capacity on Coal B: A) with Langmuir isotherm fitting; B) in relation to the replacement radius value for the selected grain class

TABLE 4

Results of CH_4 sorption measurements on Coal B

Grain class [mm]					
0.16-0.25		0.25-0.50		0.50-1.0	
R_r [cm] (eq. (8))					
0.0089		0.0174		0.0347	
P [bar]	S [$\text{cm}^3\text{CH}_4/\text{g}$]	P [bar]	S [$\text{cm}^3\text{CH}_4/\text{g}$]	P [bar]	S [$\text{cm}^3\text{CH}_4/\text{g}$]
0	0.00	0	0.00	0	0.00
1	3.54	1	3.39	1	3.13
5	10.39	5	10.18	5	9.84
15	18.41	15	18.12	15	17.76
Langmuir isotherm parameters (eq. (1))					
A [$\text{cm}^3\text{CH}_4/\text{g}$]	B [1/bar]	A [$\text{cm}^3\text{CH}_4/\text{g}$]	B [1/bar]	A [$\text{cm}^3\text{CH}_4/\text{g}$]	B [1/bar]
41.46	0.050	39.48	0.054	34.42	0.059

where: R is the equivalent grain radius; P is pressure; S is sorption capacity; B is Langmuir coefficient; A is total sorption capacity.

Similar measurements were conducted for Coal D. Equilibrium sorption points were obtained, and their values at various measurement pressures were similar, regardless of the coal grain class. The sorption capacity of CH₄ was highest at 15 bar pressure, ranging from 10.5 to 11.0 cm³/g for different grain classes. Langmuir isotherms were fitted to equilibrium sorption capacity points. The results are shown in Fig. 7A, while Fig. 7B shows the average differences in sorption capacities to the equivalent grain radius under identical pressure conditions. The observed decrease in sorption capacity correlated with the increase in replacement radius was each time 0.18-0.19 cm³CH₄/g per 0.01 cm of increase in replacement radius. The results of experimental measurements and Langmuir isotherm fitting are presented in TABLE 5.

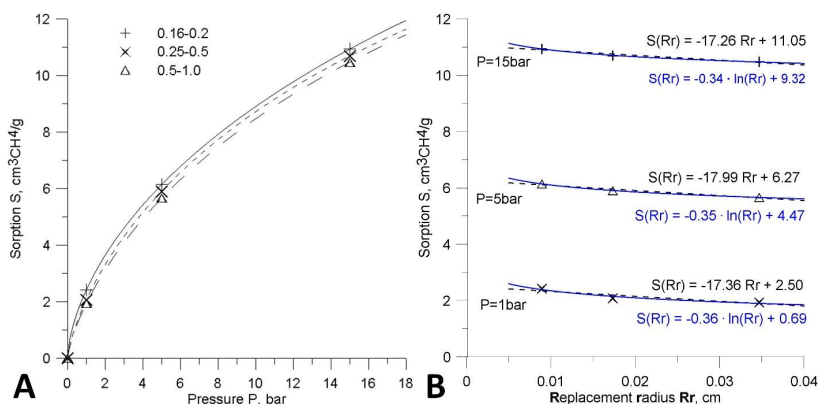


Fig. 7. CH₄ sorption capacity on Coal D: A) with Langmuir isotherm fitting; B) in relation to the replacement radius value for the selected grain class

TABLE 5

Results of CH₄ sorption measurements on Coal D

Grain class [mm]					
0.16-0.25		0.25-0.50		0.50-1.0	
<i>R_r</i> [cm]					
0.0089		0.0174		0.0347	
<i>P</i> [bar]	<i>S</i> [cm ³ CH ₄ /g]	<i>P</i> [bar]	<i>S</i> [cm ³ CH ₄ /g]	<i>P</i> [bar]	<i>S</i> [cm ³ CH ₄ /g]
0	0.00	0	0.00	0	0.00
1	2.43	1	2.07	1	1.94
5	6.14	5	5.91	5	5.66
15	10.94	15	10.70	15	10.47
Langmuir isotherm parameters					
<i>A</i> [cm ³ CH ₄ /g]	<i>B</i> [1/bar]	<i>A</i> [cm ³ CH ₄ /g]	<i>B</i> [1/bar]	<i>A</i> [cm ³ CH ₄ /g]	<i>B</i> [1/bar]
39.96	0.022	34.12	0.026	31.12	0.029

The analysis of the above measurements shows a monotonic and repeatable relationship between sorption capacity values and grain class. Both coal samples, characterised by different coal ranks, show decreasing sorption capacity at all tested pressures.

4.2. Diffusion kinetics

Diffusion kinetics studies, similar to sorption studies, were carried out in coals of three different grain classes. The process is described using the effective diffusion coefficient D_e (equation (5)). Direct measurement results for low-rank Coal B under different CH₄ pressure conditions are shown in Fig. 8.

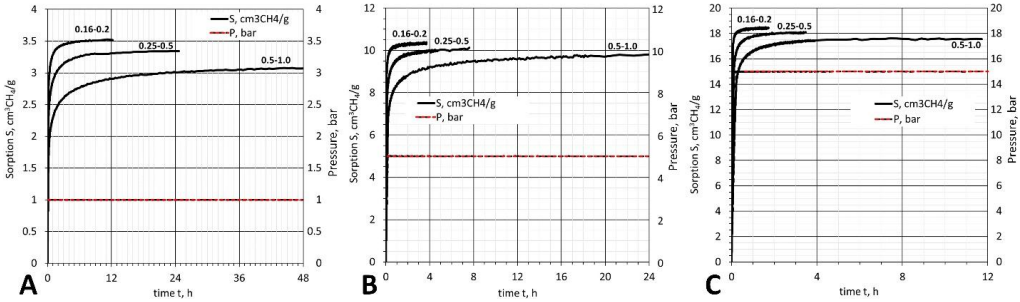


Fig. 8. CH₄ diffusion kinetics in Coal B: A) at 1 bar, B) at 5 bar, C) at 15 bar

When analysing the measurement results, it is necessary to determine the impact of the tested grain size and the measurement pressure on the CH₄ diffusion coefficient values. Fig. 9A shows the variation of D_e as a function of CH₄ pressure for three-grain classes of Coal B, represented by the replacement radius R_r . The value of this parameter depended on the measuring pressure, and its variability strongly increased, especially for higher pressures. At a pressure of 15 bar and within the largest grains, the D_e value was the highest and amounted to $9.07 \cdot 10^{-8} \text{ m}^2/\text{s}$. With a decrease in the replacement radius value, a decrease in the D_e value was recorded. This decrease was, on average, from $3.8 \cdot 10^{-8}$ to $5.8 \cdot 10^{-8} \text{ m}^2/\text{s}$ per 0.01 cm increment of the replacement radius. The value of D_e also depended on the range of the Coal B grain class and increased with the increase of the replacement radius.

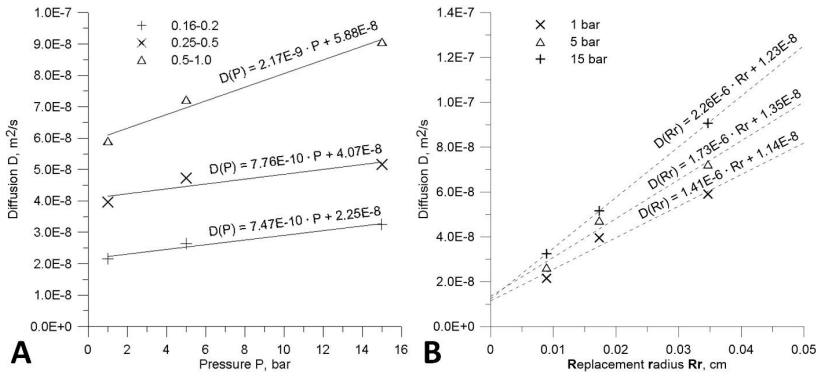


Fig. 9. CH₄ effective diffusion coefficient for Coal B: A) as a function of measurement pressure, B) as a function of replacement radius

Similarly, for Coal D, effective diffusion coefficient calculations were performed based on direct results of diffusion kinetics measurements under different pressure conditions (Fig. 10).

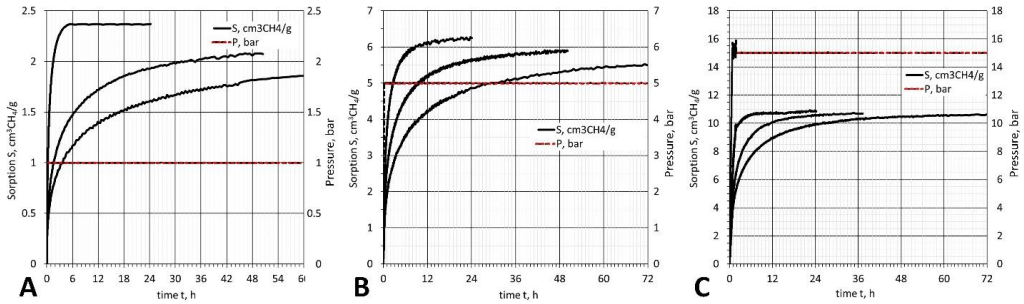


Fig. 10. CH₄ diffusion kinetics in Coal D: A) at 1 bar, B) at 5 bar, C) at 15 bar

Based on the time evolution of CH₄ transport and sorption on coal, diffusion coefficient values for Coal D were determined.

Fig. 11A shows the variability of this coefficient as a function of the replacement radius. The variability of this parameter strongly increases, especially for higher pressures. The analysis of changes in the diffusion coefficient depending on the grain class is presented in Fig. 11B. In this case, the greatest variability characterises the highest tested replacement radii.

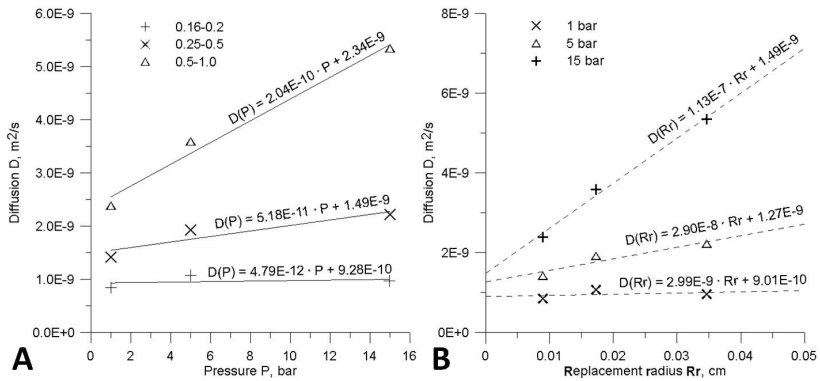


Fig. 11. CH₄ effective diffusion coefficient for Coal D: A) as a function of measurement pressure, B) as a function of replacement radius

5. Discussion

As evident from the conducted research, the sorption parameters discussed in the article are sensitive to the method of experimenting. The origins of this sensitivity are found in the assumptions of the Crank model. Providing an analytical solution for gas diffusion in a porous sorbent required many assumptions (Section 2.4), some of which pose challenges in terms of practical

application. So, which of the experiment's parameters may be critical in terms of determining the diffusion coefficient?

Challenges arise directly from the physics of the phenomenon, making it unfeasible to entirely satisfy Crank's model assumption (1) *sorption follows the linear Henry isotherm*.

There exist sorbents for which the linear isotherm is experimentally validated, but their number is limited. In the case of coal, the shape of the real methane sorption isotherm is much closer to the Langmuir model than to the Henry one. However, there is a lack of methods to derive an analytical solution for the Fick diffusion equation with a non-linear sorption isotherm.

The analysis of the real sorption isotherms for the Coal B and Coal D samples indicates that the errors attributed to assuming linearity of the sorption isotherm are the lowest at low measurement pressures. Fig. 12 illustrates the experimentally determined sorption points alongside the fitting of Langmuir and Henry isotherms. Henry's isotherms were adjusted for individual sorption points corresponding to pressures of 1, 5 and 15 bar. Each time, for higher pressures, the value of Henry's isotherm coefficient decreased progressively.

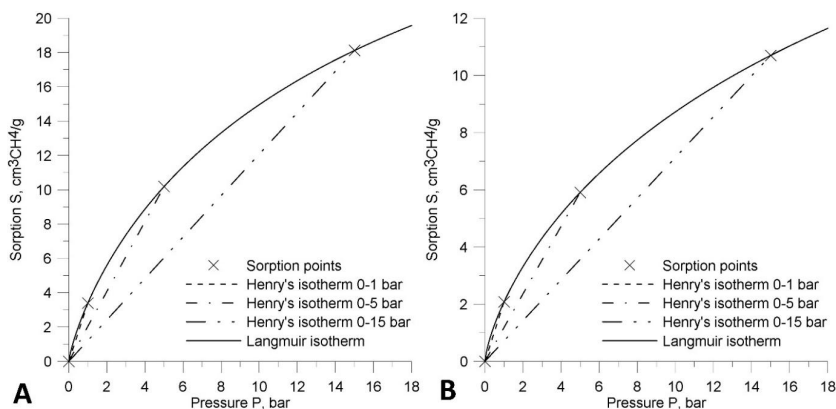


Fig. 12. Langmuir sorption isotherm with Henry's isotherms for successive sorption points: A) Coal B, B) Coal D

In the analytical solution proposed by Crank, the diffusion coefficient is referred to as the effective diffusion coefficient D_e (eq. (3)). In this context, it becomes a function of the Henry isotherm coefficient (eq. (2)), with the coefficient appearing in the denominator.

Considering the observed trend of the process, changes in individual parameters in the equation are as follows:

$$D_e = \frac{D}{1+H} \quad (10)$$

If the denominator decreases, the entire expression increases. Consequently, this stands as the primary reason for the escalation in the diffusion coefficient value with an increase in the measurement pressure.

Another assumption of the Crank model, which is challenging to fulfil, involves the step change in gas pressure at the initiation of the process: (2) *up to the initial moment $t < 0$, the grain*

is uniformly saturated and maintains equilibrium with the concentration of free gas encompassing the grain, and: (3) at $t = 0$, an abrupt alteration in gas concentration around the grain prompts the initiation of desorption and sorbate transport processes.

In this case, technical limitations lead to a limited rate of pressure changes in the reactor. Theoretically, rapid pressure changes are possible in volumetric apparatus, however, it does not often work in isobaric conditions. Consequently, maintaining constant pressure after its abrupt change becomes impossible. Additionally, a very rapid pressure change frequently results in temperature fluctuations. To conduct the measurements described in the article, a gravimetric analyzer was utilised, as explained in Chapter 2.3. This procedure involved changes in registration in the mass of the sorbent sample throughout the process. The maximum permissible pressure change in the reactor was 333 mbar/min. This means that a step change in pressure from vacuum to 1 bar took about 3 minutes. On the other hand, if the final pressure is higher, it takes much longer for the pressure to change. The consequences of technological limitations on the pressure alteration rate in the reactor can be significant. This is the case in particular if there is a step change in pressure to its high value and if the sorbate diffusion kinetics on the test sample is high compared to the rate of pressure change.

To illustrate the impact of the reactor's pressure alteration rate on the registration of diffusion kinetics, a comparison of the diffusion kinetics analysis for the same type of coal is necessary. Fig. 13 presents the results of a test involving a quasi-step pressure change from 0 to 1 bar with an analogous test with a pressure change of 0-15 bar. During the 0-1 bar pressure change (Fig. 13A), the transient phase lasted about 3 minutes. In instances where the observation of the process extends over many hours, this duration proves negligible. However, when the measuring pressure is 15 bar, it takes about 45 minutes to reach it. Figs. 13A and 13B show the different nature of the phenomena after reaching the target pressure. It is reasonable to anticipate that a more prolonged transient state will lead to an extension of the time required to attain sorption equilibrium. This duration is dictated by the duration of the diffusion process.

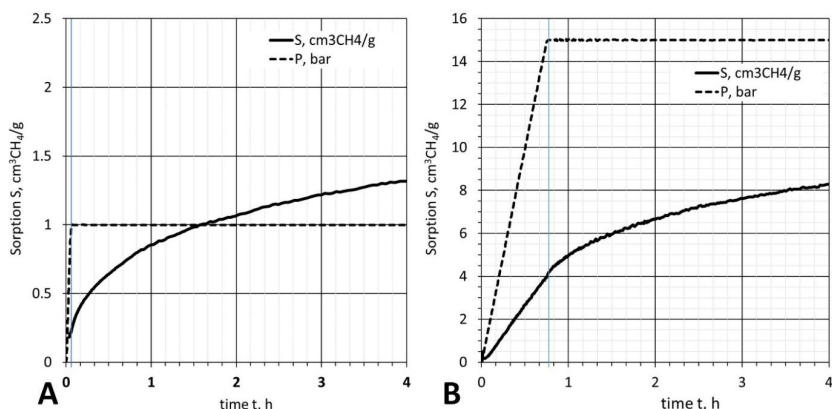


Fig. 13. The initial part of diffusion after a step change in pressure: A) 0-1 bar; B) 0-15 bar

The size of the grains also significantly influenced the experiments with the duration of the pressure change. For large grains, the process kinetics was lower, and the influence of the

transient phase during pressure alteration was small. For small grains, the process kinetics was higher, and the impact of the transient phase was correspondingly greater.

The last group of conditions concerns the assumptions of the Crank model: (4) *the coal material is homogeneous, implying the disparity in maceral composition and ash content among grains of different sizes is disregarded*, (5) *gas emanates from a spherical grain (or another regular shape)* and (6) *grain composition within the sieved class is homogeneous*.

The homogeneity of the carbon material, specifically the relationship between grain size and maceral composition, has been discussed by numerous researchers [27,56,57]. After grinding and sieving a homogeneous piece of coal sample into various grain classes, the smallest grains will be slightly different from the larger ones. This discrepancy is influenced by a factor that alters coal's susceptibility to grinding. According to [58] research, there are differences in the share of macerals in individual coal grain classes. In the examined samples, each higher grain class exhibited a higher vitrinite content and a lower inertinite content. Consequently, it can be concluded that the different percentages of the macerals also affect the analysed diffusion coefficient values, although establishing unequivocal correlations in this regard is more challenging.

6. Conclusions

The research results lead to the following conclusions:

- The sorption capacity of coal depended on the grain class of the coal material.
- The decrease in the sorption capacity of coals with the increase of their grain class was small, ranging between 0.17 and 0.2 cm³CH₄/g per 0.01 cm of the increase in the equivalent radius (in the range of the tested grain sizes).
- It was not observed that the dynamics of the reduction in the sorption capacity with the increase in grain size was dependent on the coal rank of the material.
- Diffusion kinetics were significantly affected by the chosen grain class of the carbon material.
- The diffusion coefficient's value increased as the equivalent radius increased, especially at higher pressures.
- The increments of the diffusion coefficient were higher for coal with a lower coal rank.
- The value of the diffusion coefficient showed a clear increase with the increase in pressure, and for Coal D with a higher coal rank, this increase was higher. The variability of the diffusion coefficient reached 2E-11 cm²/s for each cm of equivalent radius.

The most important conclusion drawn from this research indicates that the sorption capacity of coal and the diffusion coefficient is highly sensitive to the measurement methodology. Measurements must be carried out in a precisely defined protocol, especially when conducting qualitative interpretations of sorption parameters and the diffusion coefficient, particularly when comparing different coals. Minimization of measurement uncertainties should take into account the use of a stepwise pressure increase from UHV to a value not exceeding 1 bar to minimise the impact of sorption isotherm non-linearity on the results. The same narrow grain size class should be used each time for testing to reduce maceral inhomogeneities. It should also be ensured that the equivalent radius reduces the kinetics of the process to values much lower than the rate of pressure change in the measuring apparatus. Diffusion coefficient values are difficult to compare quantitatively due to these factors.

Acknowledgements

This work was funded by the statutory research of the Strata Mechanics Research Institute of the Polish Academy of Sciences and by the statutory research of the AGH-University of Science and Technology, Faculty of Geology, Geophysics and Environmental Protection.

Research project supported/partly supported by program „Excellence initiative – research university” for the AGH University of Krakow.

References

- [1] F. Colosimo et al., Biogenic methane in shale gas and coal bed methane: A review of current knowledge and gaps. *Int. J. Coal Geol.* **165**, 106-120 (2016). DOI: <https://doi.org/10.1016/j.coal.2016.08.011>
- [2] M. Mastalerz, A. Drobniak, D. Strapoc, W. Solano Acosta, J. Rupp, Variations in pore characteristics in high volatile bituminous coals: Implications for coal bed gas content. *Int. J. Coal Geol.* **76**, 3, 205-216 (2008). DOI: <https://doi.org/10.1016/j.coal.2008.07.006>
- [3] T.A. Moore, Coalbed methane: A review. *Int. J. Coal Geol.* **101**, 36-81 (2012). DOI: <https://doi.org/10.1016/j.coal.2012.05.011>
- [4] M. Bukowska, U. Sanetra, M. Wadas, Zonation of deposits of hard coals of different porosity in the Upper Silesian Coal Basin. *Gospodarka Surowcami Mineralnymi* **32** (1), 5-24 (2016).
- [5] D.W. van Krevelen, J. Schuyer, Węgiel. Chemia węgla i jego struktura. Publishing house: Państwowe Wydawnictwo Naukowe (1959).
- [6] L. Gao, M. Mastalerz, A. Schimmelmann, The Origin of Coalbed Methane. In *Coal Bed Methane: From Prospect to Pipeline*, Elsevier 1104 Inc., pp. 7-29 (2014). DOI: <https://doi.org/10.1016/B978-0-12-800880-5.00002-4>
- [7] D. Strapoc et al., Biogeochemistry of microbial coal-bed methane. *Annu. Rev. Earth Planet. Sci.* **39**, 617-656 (2011). DOI: <https://doi.org/10.1146/annurev-earth-040610-133343>
- [8] A. Hosseini, M. Najafi, Determination of Methane Desorption Zone for the design of a drainage borehole Pattern (Case Study: E4 Panel of the Tabas Mechanized Coal Mine, Iran), *Rudarsko-Geološko-Naftni Zbornik* **36**, 1 (2021). DOI: <https://doi.org/10.17794/rgn.2021.1.6>
- [9] M. Najafi, R. Rafiee, Development of a new index for methane drainageability of a coal seam using the fuzzy rock engineering system. *Rudarsko-Geološko-Naftni Zbornik* **34**, 4 (2019). DOI: <https://doi.org/10.17794/rgn.2019.4.4>
- [10] Q. Zhang, X. Liu, B. Nie, W. Wu, R. Wang, Methane sorption behaviour on tectonic coal under the influence of moisture. *Fuel* **327**, 125150 (2022). DOI: <https://doi.org/10.1016/j.fuel.2022.125150>
- [11] T. Gao, Q. Han, C. Deng, H. Zhang, Experimental Study on the Properties of Gas Diffusion in Various Rank Coals under Positive Pressure. *ACS Omega* **8**, 10618-10628 (2023). DOI: <https://doi.org/10.1021/acsomega.3c00716>
- [12] G.R. King, T.M. Ertekin, A survey of mathematical models related to methane production from coal seams. Part I. Empirical and equilibrium sorption models. *Proc. Coalbed Methane Symp. The Univ. of Alabama, Tuscaloosa*, 125-138 (1989).
- [13] G.R. King, T.M. Ertekin, A survey of mathematical models related to methane production from coal seams. Part II: Nonequilibrium sorption models. *Proc. Coalbed Methane Symp. The Univ. of Alabama, Tuscaloosa*, 139-155 (1989).
- [14] S. Harpalani, R.A. Schraufnagel, Measurement of parameters impacting methane recovery from coal seams. *International Journal of Mining and Geo-Engineering* **8**, 369-384 (1990). DOI: <http://doi.org/10.1007/BF00920648>
- [15] S. Harpalani, R.A. Schraufnagel, Shrinkage of coal matrix with release of gas and its impact on permeability of coal. *Fuel* **69**, 551-556 (1990). DOI: [https://doi.org/10.1016/0016-2361\(90\)90137-F](https://doi.org/10.1016/0016-2361(90)90137-F)
- [16] P.J. Crosdale, B.B. Beamish, M. Valix, Coalbed methane sorption related to coal Composition. *International Journal of Coal Geology* **35**, 147-158 (1998). DOI: [https://doi.org/10.1016/S0166-5162\(97\)00015-3](https://doi.org/10.1016/S0166-5162(97)00015-3)
- [17] T. Hobler, *Dyfuzyjny ruch masy i absorber*. Publishing house: Wydawnictwo Naukowo-Techniczne (1976).
- [18] P. Naveen, M. Asif, K. Ojha, D.C. Panigrahi, H.B. Vuthaluru, Sorption Kinetics of CH₄ and CO₂ Diffusion in Coal: Theoretical and Experimental Study. *Energy Fuels* **31**, 6825-6837 (2017). DOI: <https://doi.org/10.1021/acs.energyfuels.7b00721>

- [19] F. Han, A. Busch, B.M. Krooss, Z. Liu, J. Yang, CH₄ and CO₂ sorption isotherms and kinetics for different size fractions of two coals. *Fuel* **108**, 137-142 (2013). DOI: <https://doi.org/10.1016/j.fuel.2011.12.014>
- [20] H. Long, H. Lin, M. Yan, Y. Bai, X. Tong, X. Kong, S. Li, Adsorption and diffusion characteristics of CH₄, CO₂, and N₂ in micropores and mesopores of bituminous coal: Molecular dynamics. *Fuel* **292**, 120268 (2021). DOI: <https://doi.org/10.1016/j.fuel.2021.120268>
- [21] Y. Xu, X. Chen, J. Yu, Experimental study of the radial multi-scale dynamic diffusion model for gas-bearing coal. *Mining of Mineral Deposits* **16** (4), 80-86 (2022). DOI: <https://doi.org/10.33271/mining16.04.080>
- [22] Z. Pan, L.D. Connell, M. Camilleri, L. Connelly, Effects of matrix moisture on gas diffusion and flow in coal. *Fuel* **89** (11), 3207-3217 (2010). DOI: <https://doi.org/10.1016/j.fuel.2010.05.038>
- [23] W. Yang, L. Wang, K. Yang, S. Fu, C. Tian, R. Pan, Molecular insights on influence of CO₂ on CH₄ adsorption and diffusion behaviour in coal under ultrasonic excitation. *Fuel* **355**, 129519 (2024). DOI: <https://doi.org/10.1016/j.fuel.2023.129519>
- [24] J. Zhang, Experimental Study and Modeling for CO₂ Diffusion in Coals with Different Particle Sizes: Based on Gas Absorption (Imbibition) and Pore Structure. *Energy & Fuels* **30** (1), 531-543 (2016). DOI: <https://doi.org/10.1021/acs.energyfuels.5b02546>
- [25] X. Jian, P. Guan, W. Zhang, Carbon dioxide sorption and diffusion in coals: Experimental investigation and modelling. *Science China Earth Sciences* **55** (4), 633-643 (2012). DOI: <https://doi.org/10.1007/s11430-011-4272-4>
- [26] A. Ciembroniewicz, A. Marecka, Kinetics of CO₂ sorption for two Polish hard coals. *Fuel* **72** (3), 405-408 (1993). DOI: [https://doi.org/10.1016/0016-2361\(93\)90062-7](https://doi.org/10.1016/0016-2361(93)90062-7)
- [27] C.R. Clarkson, R.M. Bustin, The effect of pore structure and gas pressure upon the transport properties of coal: a laboratory and modelling study. 2. Adsorption rate modelling. *Fuel* **78** (11), 1345-1362 (1999). DOI: [https://doi.org/10.1016/S0016-2361\(99\)00056-3](https://doi.org/10.1016/S0016-2361(99)00056-3)
- [28] G. Staib, R. Sakurovs, E.M.A. Gray, A pressure and concentration dependence of CO₂ diffusion in two Australian bituminous coals. *International Journal of Coal Geology* **116-117**, 106-116 (2013). DOI: <https://doi.org/10.1016/j.coal.2013.07.005>
- [29] X. Cui, R.M. Bustin, G. Dipple, Selective transport of CO₂, CH₄, and N₂ in coals: insights from modelling of experimental gas adsorption data. *Fuel* **83** (3), 293-303 (2004). DOI: <https://doi.org/10.1016/j.fuel.2003.09.001>
- [30] A. Liu, P. Liu, S. Liu, Gas diffusion coefficient estimation of coal: A dimensionless numerical method and its experimental validation. *International Journal of Heat and Mass Transfer* **327**, 120336 (2020). DOI: <https://doi.org/10.1016/j.ijheatmasstransfer.2020.120336>
- [31] G. Wang, T. Ren, Q. Qi, J. Lin, Q. Liu, J. Zhang, Determining the diffusion coefficient of gas diffusion in coal: Development of numerical solution. *Fuel* **196**, 47-58 (2017). DOI: <https://doi.org/10.1016/j.fuel.2017.01.077>
- [32] D. Charrière, Z. Pokryszka, P. Behra, Effect of pressure and temperature on diffusion of CO₂ and CH₄ into coal from the Lorraine basin (France). *International Journal of Coal Geology* **81** (4), 373-380 (2010). DOI: <https://doi.org/10.1016/j.coal.2009.03.007>
- [33] Y. Zhang, W. Xing, S. Liu, Y. Liu, M. Yang, J. Zhao, Y. Song, Pure methane, carbon dioxide, and nitrogen adsorption on anthracite from China over a wide range of pressures and temperatures: experiments and modelling. *RSC Advances* **5** (65), 52612-52623 (2015). DOI: <https://doi.org/10.1039/C5RA05745K>
- [34] H. Hu, L. Du, Y. Xing, X. Li, Detailed study on self- and multicomponent diffusion of CO₂-CH₄ gas mixture in coal by molecular simulation. *Fuel* **187**, 220-228 (2017). DOI: <https://doi.org/10.1016/j.fuel.2016.09.056>
- [35] C. Fan, D. Elsworth, S. Li, L. Zhou, Z. Yang, Y. Song, Thermo-hydro-mechanical-chemical couplings controlling CH₄ production and CO₂ sequestration in enhanced coalbed methane recovery. *Energy* **173**, 1054-1077 (2019). DOI: <https://doi.org/10.1016/j.energy.2019.02.126>
- [36] Y. Zhao, Y. Feng, X. Zhang, Molecular simulation of CO₂/CH₄ self- and transport diffusion coefficients in coal. *Fuel* **165**, 19-27 (2016). DOI: <https://doi.org/10.1016/j.fuel.2015.10.035>
- [37] A. Keshavarz, R. Sakurovs, M. Grigore, M. Sayyafzadeh, Effect of maceral composition and coal rank on gas diffusion in Australian coals. *International Journal of Coal Geology* **173**, 65-75 (2017). DOI: <https://doi.org/10.1016/j.coal.2017.02.005>
- [38] B. Dutka, K. Godyń, Coalification as a Process Determining the Methane Adsorption Ability of Coal Seams. *Archives of Mining Sciences* **66** (2), 181-195 (2021). DOI: <https://doi.org/10.24425/ams.2021.137455>

- [39] M. Karbownik, J. Krawczyk, T. Schlieter, The Unipore and Bidisperse Diffusion Models for Methane in Hard Coal Solid Structures Related to the Conditions in the Upper Silesian Coal Basin. *Archives of Mining Sciences* **65** (3), 591-603 (2020). DOI: <https://doi.org/10.24425/ams.2020.134136>
- [40] K. Godyń, B. Dutka, The impact of the degree of coalification on the sorption capacity of coals from the Zofiówka Monocline. *Archives of Mining Sciences* **63** (3), 727-746 (2018). DOI: <https://doi.org/10.24425/123694>
- [41] T. Adsul, S. Ghosh, S. Kumar, B. Tiwari, S. Dutta, A.K. Varma, Biogeochemical Controls on Methane Generation: A Review on Indian Coal Resources. *Minerals* **13** (5), 695 (2023). DOI: <https://doi.org/10.3390/min13050695>
- [42] C. Laxminarayana, P.J. Crosdale, Role of coal type and rank on methane sorption characteristics of Bowen Basin, Australia coals. *International Journal of Coal Geology* **40** (4), 309-325 (1999). DOI: [https://doi.org/10.1016/S0166-5162\(99\)00005-1](https://doi.org/10.1016/S0166-5162(99)00005-1)
- [43] H. Koptoń, Impact Assessment of Sorption Properties of Coal on Methane Emissions Into Longwall Working. *Archives of Mining Sciences* **65** (3), 605-625 (2020). DOI: <https://doi.org/10.24425/ams.2020.134137>
- [44] M. Gawor, N. Skoczylas, A. Pajdak, M. Kudasik, Nonlinear and Linear Equation of Gas Diffusion in Coal – Theory and Applications. *Applied Sciences* **11**, 5130 (2021). DOI: <https://doi.org/10.3390/app11115130>
- [45] W. Zhao, Y. Cheng, Z. Pan, K. Wang, S. Liu, Gas diffusion in coal particles: A review of mathematical models and their applications. *Fuel* **252**, 77-100 (2019). DOI: <https://doi.org/10.1016/j.fuel.2019.04.065>
- [46] N. Skoczylas, J. Topolnicki, The coal-gas system – the effective diffusion coefficient. *International Journal of Oil, Gas and Coal Technology* **12** (4), 412 (2016). DOI: <https://doi.org/10.1504/IJOGCT.2016.077300>
- [47] J. Crank, *The Mathematics of diffusion*. 2nd ed. Oxford Univ. Press, London (1975).
- [48] N. Skoczylas, A. Pajdak, M. Kudasik, L. Braga, CH₄ and CO₂ sorption and diffusion carried out in various temperatures on hard coal samples of various degrees of coalification (NCN nr 2016/23/B/ST8/00744). *Journal of Natural Gas Science and Engineering* **81**, 103449 (2020). DOI: <https://doi.org/10.1016/j.jngse.2020.103449>
- [49] M. Wierzbicki, A. Pajdak, P. Baran, K. Zarębska, Isosteric heat of sorption of methane on selected hard coals. *Przemysł Chemiczny* **98/4**, 625-629 (2019). DOI: <http://dx.doi.org/10.15199/62.2019.4.22>
- [50] M. Kudasik, The manometric sorptomat – an innovative volumetric instrument for sorption measurements performed under isobaric conditions. *Measurement Science and Technology* **27** (3), 035903 (2016). DOI: <https://doi.org/10.1088/0957-0233/27/3/035903>
- [51] C. Li, H. Xue, P. Hu, C. Guan, W. Liu, Effect of stress on the diffusion kinetics of methane during gas desorption in coal matrix under different equilibrium pressures. *Journal of Geophysics and Engineering* **15** (3), 841-851 (2018). DOI: <https://doi.org/10.1088/1742-2140/aaa8ad>
- [52] A. Pajdak, Parameters of N₂ and CO₂ adsorption onto coal at various temperatures. In *Proceedings of the 18th International Multidisciplinary Scientific Geoconference SGEM, Albena, Bulgaria*, p. 633-640 (2018).
- [53] M. Skiba, M. Młynarczuk, Estimation of coal's sorption parameters using artificial neural networks. *Materials* **13** (23), 5422 (2020). DOI: <https://doi.org/10.3390/ma13235422>
- [54] K. Godyń, B. Dutka, M. Chuchro, M. Młynarczuk, Synergy of Parameters Determining the Optimal Properties of Coal as a Natural Sorbent. *Energies* **13** (8), 1967 (2020). DOI: <https://doi.org/10.3390/en13081967>
- [55] M. Kudasik, Results of comparative sorption studies of the coal-methane system carried out by means of an original volumetric device and a reference gravimetric instrument. *Adsorption* **23** (4), 613-626 (2017). DOI: <https://doi.org/10.1007/s10450-017-9881-6>
- [56] C.R. Clarkson, R.M. Bustin, Binary gas adsorption/desorption isotherms: effect of moisture and coal composition upon carbon dioxide selectivity over methane. *International Journal of Coal Geology* **42**, 241-271 (2000). DOI: [https://doi.org/10.1016/S0166-5162\(99\)00032-4](https://doi.org/10.1016/S0166-5162(99)00032-4)
- [57] C.R. Clarkson, PhD thesis, The effect of coal composition, moisture content, and pore volume distribution upon single and binary gas equilibrium and nonequilibrium adsorption: implications for gas content determination, The University of British Columbia, Vancouver, Canada (1998).
- [58] C.K. Man, J. Jacobs, J.R. Gibbins, Selective maceral enrichment during grinding and effect of particle size on coal devolatilisation yields. *Fuel Processing Technology* **56** (3), 215-227 (1998). DOI: [https://doi.org/10.1016/S0378-3820\(98\)00060-5](https://doi.org/10.1016/S0378-3820(98)00060-5)